JSSS
Journal of Sensors
and Sensor Systems
Open Access

Aerosol-deposited BaFe$_{0.7}$Ta$_{0.3}$O$_{3-\delta}$ for nitrogen monoxide and temperature-independent oxygen sensing

M. Bektas, D. Hanft, D. Schönauer-Kamin, T. Stöcker, G. Hagen, and R. Moos

Department of Functional Materials, University of Bayreuth, 95447 Bayreuth, Germany

Correspondence to: R. Moos (functional.materials@uni-bayreuth.de)

Abstract. The gas sensing properties of resistive gas sensors of BaFe$_{0.7}$Ta$_{0.3}$O$_{3-\delta}$ (BFT30) prepared by the so-called aerosol deposition method, a method to manufacture dense ceramic films at room temperature, were investigated. The electrical response of the films was investigated first under various oxygen concentrations and in a wide temperature range between 350 and 900 °C. Between 700 and 900 °C, the conductivity of BaFe$_{0.7}$Ta$_{0.3}$O$_{3-\delta}$ (BFT30) depends on the oxygen concentration with a slope of almost 1/4 in the double-logarithmic plot vs. oxygen partial pressure. In addition, the sensor response is temperature independent. BFT30 responds fast and reproducibly to changing oxygen partial pressures even at 350 °C. The cross-sensitivity has been investigated in environments with various gases (C$_3$H$_8$, NO, NO$_2$, H$_2$, CO, CO$_2$, and H$_2$O) in synthetic air between 350 and 800 °C. BFT30 exhibits good sensing properties to NO between 350 and 400 °C in the range from 1.5 to 2000 ppm with a high selectivity to the other investigated gas species. Thus this semiconducting ceramic material is a good candidate for a temperature-independent oxygen sensor at high temperatures with the application in exhausts and for a selective nitrogen monoxide (NO) sensor at low temperatures for air quality monitoring.

1 Introduction

Selective oxygen sensors should respond only to changes in the oxygen partial pressure (pO$_2$) but neither to temperature variations nor to other noise factors like interfering gas components (Moseley and Williams, 1989). At the same time, oxygen sensors have to withstand harsh ambient conditions (Alkemade and Schumann, 2006; Moos et al., 2011). Besides established zirconia-based sensors (Riegel et al., 2002; Ivers-Tiffée et al., 2001), semiconducting oxides are often discussed as suitable sensor materials for that purpose (Gerblinger et al., 1995; Fleischer and Meixner, 1991). Since their pO$_2$-dependent defect disorder leads to changes in their conductivity, simple resistance measurements can indicate oxygen concentrations in exhausts or in flue gases. Due to their high melting and decomposition temperatures, perovskite oxides were extensively studied. Besides that, the perovskite structure has doping flexibility to optimize sensor performance for particular applications (Fergus, 2007). Up to now, only a few materials have been found that show a low or even negligible temperature dependency of conductivity like Co$_{1-x}$Mg$_x$O (Park and Logothetis, 1977),

SrMg$_{0.4}$Ti$_{0.6}$O$_3$ (Yu et al., 1986), La$_2$CuO$_4$ (Blase et al., 1997), and SrTi$_{0.65}$Fe$_{0.35}$O$_{3-\delta}$ (STF35) (Menesklou et al., 1999; Moos et al., 2003). Originally, Williams et al. (1982) suggested STF as a temperature-independent oxygen sensor material. Over the past decade, it has attracted a lot of attention from the research point of view. Unfortunately, STF has some problems in real exhaust applications like sulfur oxide poisoning (Rettig et al., 2004) and instability under fuel-rich conditions. Moseley and Williams (1989) suggested BaFe$_{0.8}$Ta$_{0.2}$O$_{3-\delta}$ as a temperature-independent oxygen sensor material. In our previous study, the oxygen sensing properties of bulk ceramic samples of the entire series of BaFe$_{1-x}$Ta$_x$O$_{3-\delta}$ (BFT) with $0.2 \leq x \leq 0.7$ were investigated as a function of pO$_2$ and temperature between 400 and 900 °C (Bektas et al., 2014). The conductivity of BaFe$_{0.7}$Ta$_{0.3}$O$_{3-\delta}$ (BFT30) responds rapidly and reproducibly to oxygen partial pressure changes, and it shows a negligible temperature dependency between 800 and 900 °C.

So far, many resistive thick film oxygen sensors have been produced by screen printing method, e.g., Mg-doped SrTiO$_3$ (Zhou et al., 1997), SrTi$_{0.65}$Fe$_{0.35}$O$_{3-\delta}$ (Menesklou

et al., 1999), LaCu$_{0.3}$Fe$_{0.7}$O$_{3-\delta}$, (Sahner et al., 2006a) and La$_{0.05}$Sr$_{0.95}$Ti$_{0.65}$Fe$_{0.35}$O$_{3-\delta}$ (LSTF) (Sahner et al., 2006b). Moos et al. (2003) investigated LSTF thick films that were produced by screen printing method as temperature-independent resistive oxygen sensor. The authors found that the highest possible sintering temperature is 1100 °C, since otherwise the thick films can deteriorate during sintering due to reactions between the sensitive film and the alumina substrate. To avoid such reactions and to produce stable LSTF thick films, a screen-printed SrAl$_2$O$_4$ diffusion barrier layer has to be inserted between gas sensitive layer and alumina substrate (Moos et al., 2003; Sahner et al., 2005). In order to overcome this drawback, Sahner et al. (2009) suggested applying the so-called aerosol deposition method (ADM) for the preparation of the sensor films. ADM is a novel and powerful method to manufacture dense ceramic layers at room temperature directly from ceramic powders. ADM is a completely cold method, at which neither carrier gases, nor powders or substrates must be heated (Akedo, 2006). Akedo (2006) suggested that, during the deposition process, submicron ceramic particles in a carrier gas are driven by a pressure difference between an aerosol and a coating chamber. These particles are accelerated by a nozzle to several hundred meters per second and ejected onto a substrate where they form a dense coating with nanosized particles (Akedo, 2008; Lebedev et al., 2005). So, the great advantage of ADM is that no diffusion barrier layer is required since interactions between film and substrate cannot occur, as no high temperature step is involved. Initial tests for STF clearly showed that the unique temperature-independent conductivity behavior can be fully retained using ADM (Sahner et al., 2009).

This study investigates the oxygen sensing properties of the thick film resistive sensor material BaFe$_{0.7}$Ta$_{0.3}$O$_{3-\delta}$, processed by ADM. In contrast to earlier studies of STF and BFT, also the temperature range down to 350 °C is investigated as well as influences of interfering exhaust gas components like NO, NO$_2$, H$_2$, CO, CO$_2$, and H$_2$O.

2 Experimental

BaFe$_{0.7}$Ta$_{0.3}$O$_{3-\delta}$ powder was prepared from commercially available precursor powders BaCO$_3$ (Merck), Fe$_2$O$_3$ (Alfa Aesar, 99 %) and Ta$_2$O$_5$ (Alfa Aesar, 99 %). Conventional mixed-oxide technique was used to produce BFT30 powder for ADM. To obtain homogeneous mixtures, the precursor powders were ball-milled in cyclohexane for 4 h and dried in air for 1 day. The powders were then calcined at 1350 °C for 15 h. In order to reduce the particle size, the powders were milled again and dried in air atmosphere. Finally, to remove large agglomerates the dried powders were sieved with 90 μm meshes. Before aerosol deposition, the powder was dried again for 1 day at 200 °C.
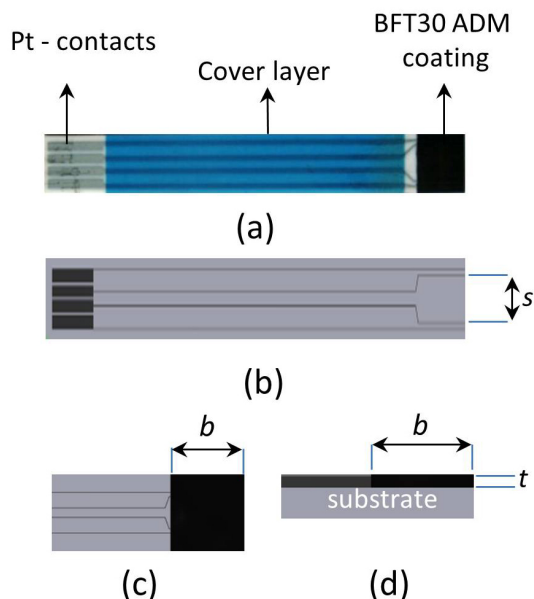

Figure 1. Sketch of the sensor setup, **(a)** top view of sensor showing Pt contacts, cover layer and BFT30 ADM coating, **(b)**, **(c)** and **(d)** indicating the dimension for the calculation of the conductivity.

Before starting the aerosol deposition, alumina substrates with four screen-printed platinum electrodes (electrode space s) were prepared. Four platinum wires were contacted to the electrodes with platinum paste (LPA 88–11S, Heraeus). The contacted substrates were fired in air at 1000 °C for 10 min. On this transducer, the ADM layer was applied. Figure 1 sketches the setup and explains the meaning of the variables that appear in Eq. (1).

The aerosol deposition experiment setup has already been depicted in detail by Sahner et al. (2009). Nitrogen served as the carrier gas and the gas flow rate was 4 L min^{-1}. The shaking frequency of the vibrating table was set to 400 min^{-1}. The distance between nozzle and substrate was adjusted to 4 mm. The substrate holder moved with a velocity 1 mm s^{-1}. By adjusting the coating time, samples with a thickness, t, of around 12 μm were produced. In order to increase electrical and mechanical properties of coated samples, they were heat-treated at 950 °C for 2 h. The temperature of this "degreening process" is far below the typical sintering temperatures of about 1350 °C but a little higher as the highest sensor operation temperature of 900 °C. This degreening process was selected to obtain reproducible results.

Phase purity of BFT30 powder was investigated by an X-Ray diffraction (PANalytical Xpert Pro) at room temperature using CuK$_\alpha$ radiation (1.541874 Å). Micrographs of sensors were determined by scanning electron microscope (SEM; Zeiss Ultra plus FE-SEM). For the gas sensing measurements, a four-wire technique with a Keithley 2700 digital multimeter in the offset-compensated resistance measuring mode was used. The ADM-coated samples were mounted on
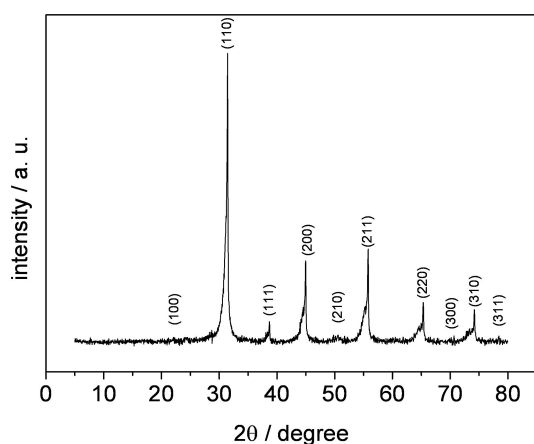
Figure 2. XRD pattern of the BFT30 powder as it was used for the ADM process.

Figure 3. SEM images of ADM-coated BFT30 sensor **(a)** top view, **(b)** cross-section micrograph.

a sample holder and inserted into a tubular furnace. The oxygen concentration was varied in the range from 1 to 100 % ($pO_2 \approx 0.01$–1 bar) in the temperature range from 350 to 900 °C. The total gas flow was adjusted to 200 mL min^{-1}. The cross-sensitivity of coated samples was investigated in environments with various gases (C_3H_8, NO, NO_2, H_2, CO, CO_2, and H_2O) in flowing synthetic air between 350 and 800 °C. The conductivity was calculated from the resistance, R, according to Eq. (1):

$$\sigma = \frac{1}{R} \cdot \frac{s}{b \cdot t}. \tag{1}$$

3 Results and discussion

3.1 Characterization

Figure 2 shows the X-ray diffraction (XRD) graph of the BaFe$_{0.7}$Ta$_{0.3}$O$_{3-\delta}$ (BFT30) precursor powder that was calcined at 1350 °C for 15 h. The XRD patterns indicate that the phase structure of BFT30 has a tetragonal to cubic perovskite phase transition when calcined at 1350 °C. In other words, the sensor material has a non-cubic perovskite phase (as indexed). Second phases cannot be observed.

The BFT30 powders were ADM-processed onto substrates as described above. One specimen was cut and prepared for SEM micrographs. A top view image and a cross section (polished) are shown in Fig. 3a and b, respectively. The resulting film is found to be dense and homogeneous with a film thickness of about 12 μm. A closer look into the microstructure revealed a crystallite size in the range of some tens of nanometers, as it is typical for ADM-processed ceramic materials since the grains fracture during impaction on the substrate (Lebedev et al., 2005; Akedo, 2006).
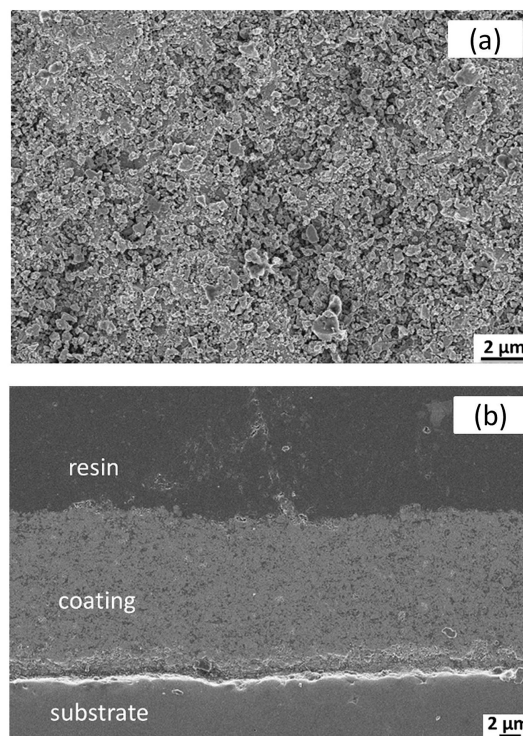
3.2 Oxygen sensing properties

The oxygen sensing properties of BFT30 thick films were investigated by varying gradually the oxygen partial pressure from 10^{-2} to 1 bar at a fixed temperature. The oxygen concentration was held for 20 min at each step. The conductivity reached a stable final value within these 20 min as shown for 900 °C in Fig. 4a, and an almost stable final value for 350 °C in Fig. 4b. Similar results were observed for BFT30 bulk samples between 500 and 900 °C in our previous study (Bektas et al., 2014). It can be seen from Fig. 4b that an ADM-processed BFT30 sensor shows a fast and reversible response to oxygen partial pressure changes even at low temperatures of 350 °C. At such a low temperature, one usually cannot expect a full equilibration of the oxygen equilibrium as given by defect chemical constants, due to the usually slow oxygen kinetics at low temperatures. However, if oxygen diffusion within the crystallite is the time-limiting step of the sensor response, the oxygen equilibration time should be proportional to the square of the grain size (Schönauer, 1991). Therefore, the nanosized crystallite structure may explain this unexpected fast response.

In Fig. 5 the conductivity of the BFT30 sensors is shown in a double-logarithmic representation vs. oxygen partial pressure. Since BFT30 is a p type conductor, its conductivity increases with increasing oxygen partial pressure. Very often, and in agreement with defect chemistry (Merkle and Maier,
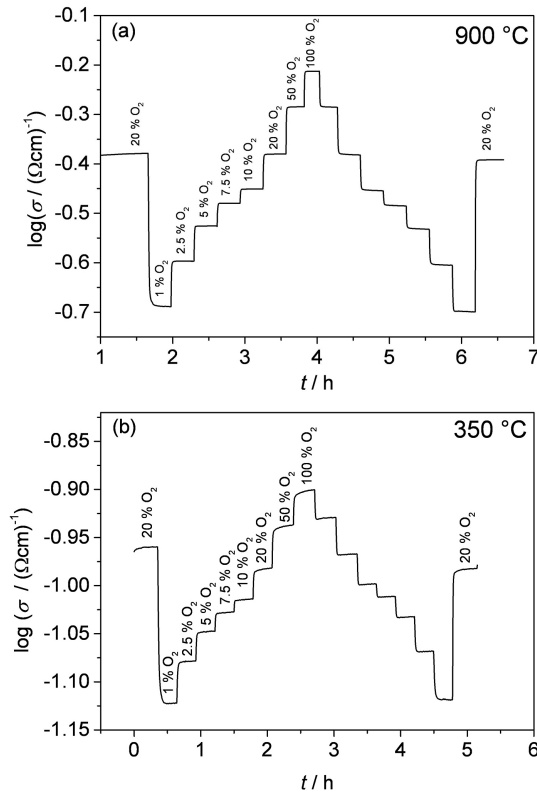
www.j-sens-sens-syst.net/3/223/2014/

J. Sens. Sens. Syst., 3, 223–229, 2014

Figure 4. Conductivity of the BFT30 sensor as a function of pO$_2$ (a) at 900 °C and (b) at 350 °C.

2008), one finds a behavior for the conductivity according to Eq. (2), with the exponent m being in the range between 1/6 and 1/4:

$$\sigma = \text{const.} \times p\text{O}_2{}^m. \tag{2}$$

In a double-logarithmic representation, the sensitivity, S_{O_2}, is the slope of the curve (Eq. 3):

$$S_{\text{O}_2} = \frac{\text{d lg}(\sigma)}{\text{d lg}(p\text{O}_2)} = m. \tag{3}$$

The sensitivity of the sensor increases with temperature from 0.21 at 600 °C to 0.24 between 700 and 900 °C. It is remarkable that between 700 and 900 °C the curves are almost identical, indicating an almost perfect temperature independency. Only below 700 °C, the sensor becomes temperature dependent. According to Bektas et al. (2014), the increasing tantalum content reduces the amount of oxygen vacancies. The oxygen deficiency, δ, moves from 0.5 towards zero. At the same time, the conductivity decreases with tantalum content, x, since the holes are compensated. The tantalum stabilizes the phase by reducing oxygen deficiency. This may lead to the temperature independency.
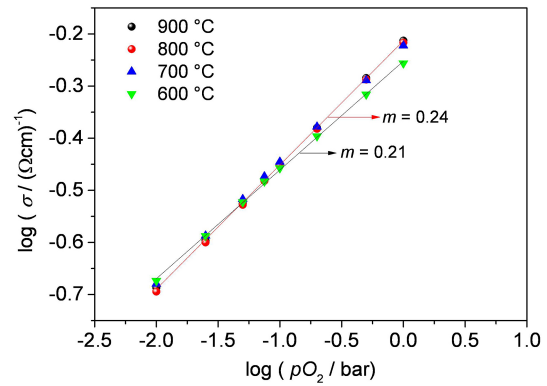

Figure 5. Double-logarithmic plot of conductivity vs. oxygen partial pressure for a BFT30 ADM-coated sensor. Please note that the curves of 700, 800, and 900 °C can hardly be distinguished.
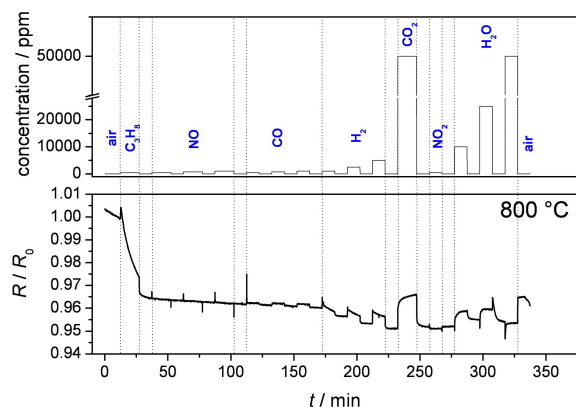
3.3 Sensitivities to the other gases

In order to determine the behavior of BFT30 ADM-coated thick film sensors to other exhaust components, the resistance of the sensor was measured under the presence of defined concentrations of the following components: C$_3$H$_8$ (500 ppm), NO (1000 ppm), NO$_2$ (500 ppm), H$_2$ (5000 ppm), CO (1000 ppm), CO$_2$ (5 %), and H$_2$O (5 %) between 350 and 800 °C. Base gas was synthetic air. The resistances, R, were measured, and together with the values in base gas, R_0, the response to each component, $S_{\text{component}}$, was calculated according to Eq. (4). The results are summarized in Table 1 for all investigated temperatures.

$$S_{\text{component}} = \frac{R - R_0}{R_0}. \tag{4}$$

One can see from Table 1 that the sensor responds only in a negligible way to other exhaust components above 600 and 800 °C. This has been expected, since we assume at such high temperatures a full equilibration between oxide ceramic material and oxygen atmospheres, an effect that becomes clear if one considers that both the oxygen incorporation kinetics and the oxygen (vacancy) diffusion are fast at such temperatures. Therefore, at high temperatures between 600 and 800 °C the resistance of BFT30 ADM-coated samples depends mainly on the oxygen partial pressure. The dynamic response curve (here expressed as the normalized resistance R/R_0) from the cross-sensitivity test at 800 °C confirms this (Fig. 6). One can see that most gases have a negligible influence on the sensor response. Even at lower temperature, only minor cross-effects were found, with sensitivities mainly below 10 %. However, a prominent influence of NO at 400 and 350 °C is observed, with only a marginal effect of NO$_2$. This astonishing behavior may offer the chance to use BFT as a resistive NO sensor for air quality control or other applications where the oxygen concentration remains constant. This will be investigated in the next paragraph more in detail.
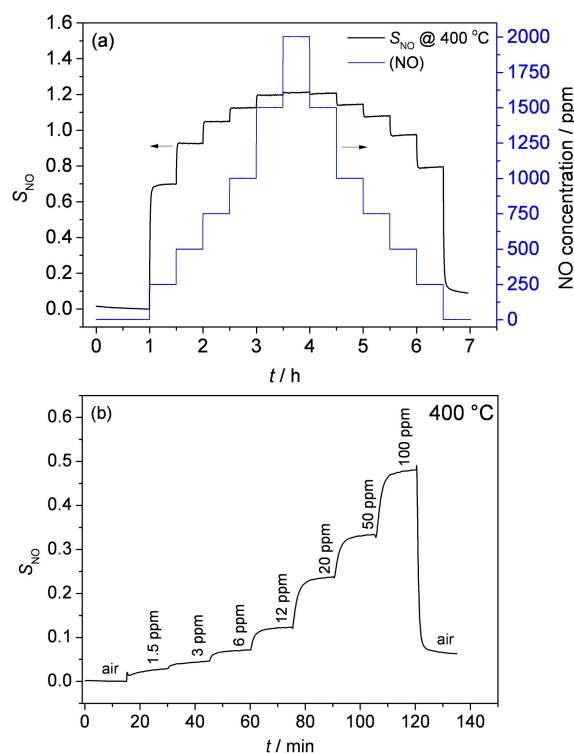
Table 1. Response, $S_{\text{component}}$, as defined in Eq. (4) of the BFT30 ADM thick film sensor to other exhaust components.

$T/°C$	$S_{C_3H_8}/\%$	$S_{NO}/\%$	$S_{NO_2}/\%$	$S_{H_2}/\%$	$S_{CO}/\%$	$S_{CO_2}/\%$	$S_{H_2O}/\%$
350	51.1	234.1	15.3	5.58	1.06	0.21	9.82
400	12.5	119.4	15.0	4.48	2.89	1.52	8.82
600	2.77	2.81	1.13	1.28	2.84	8.66	2.97
800	2.63	0	0.11	0.33	1.11	1.55	1.20

Figure 6. Cross-sensitivity result of a BFT30 ADM-coated sensor at 800 °C (base gas is synthetic air).

3.4 NO sensing properties

According to today's increasing environmental standards, toxic and harmful gases such as NO$_x$ (NO and NO$_2$), H$_2$S, CO, and NH$_3$ that are dangerous for environment and/or human health have to be detected by highly selective gas sensors (Huusko et al., 1993; Satake et al., 1994; Marr et al., 2014). Besides that, for automotive in-cabin applications NO$_x$ sensors may be used for air quality control, by determining the amount of NO$_x$ in the passenger compartment (Kim et al., 2008). In these cases, the oxygen concentration of the ambience remains almost constant. With respect to the high NO response, it may therefore make sense to investigate whether the ADM-processed BFT sensor can be used as an NO sensor. Therefore, response to NO was investigated more in detail. According to Table 1, 400 °C seems to be the first choice, since at that temperature the effect of NO exceeds all others largely. Figure 7a shows the normalized resistance, R/R_0, of a BFT30 ADM-coated sensor under the presence of NO in concentrations between 250 and 2000 ppm in flowing synthetic air. As can be seen, the sensor has a fast, stable and reversible response to NO. Especially low NO concentrations seem to affect the sensor response strongly. At higher NO concentrations, a saturation behavior occurs. Therefore, lower NO concentrations were observed. Figure 7b shows the NO dependence of the ADM BFT30 sensor at lower NO concentrations from 1.5 to 100 ppm. The absolute lower dosing limit in the used test bench is 1.5 ppm. Again, one finds a

Figure 7. Response of an ADM BFT30 sensor at 400 °C. **(a)** NO concentrations from 250 to 2000 ppm, **(b)** NO concentrations between 1.5 and 100 ppm.

fast response but with some irregularities at 1.5 ppm NO that may originate from mixing problems in the test bench. During recovery, it takes some time until the steady-state value is reached. Nevertheless, we consider this a promising approach, especially due to the high selectivity.

These promising results shall be compared with literature data for other semiconducting NO sensors. Sayago et al. (1995) studied the sensitivity of undoped, Pt-, In- and Al-doped SnO$_2$ as NO$_x$ and CO sensors. They found response times of around 20 min for Al- or In-doped SnO$_2$ sensors when exposed to NO$_x$. Akiyama et al. (1993) investigated WO$_3$ as NO and NO$_2$ sensor material in the temperature range between 200 and 500 °C. They found that WO$_3$ responds quite well to NO and NO$_2$ in air. According to their suggestions, the NO sensitivity can be further promoted by electrode metals and addition of noble metals like Ru and

Au. Besides that, Penza et al. (1998) investigated WO$_3$-based thin film sensor devices with activator layers of Pd, Pt and Au. The response time to NO for WO$_3$: Pt sensors decreased to 2.8 min. Despite that, one has to state that the response of most other materials to NO is higher, and the ADM BFT30 sensor has a faster response to NO (less than 1 min) and a good selectivity to many gases that are relevant for air quality monitoring. Especially NO, CO and H$_2$O are relevant in this respect (Wiegleb and Heitbaum, 1994; Kim et al., 2008).

4 Conclusions

BFT30 dense and thick film sensors were manufactured by the aerosol deposition method at room temperature. The resistance change of the sensors was investigated as a function of oxygen partial pressure and temperature. BFT30 sensors show a fast, reproducible, and temperature-independent response to pO$_2$ between 700 and 900 °C. Cross-sensitivity tests have been conducted under interfering gases in synthetic air. The results demonstrate that the sensor has no crucial sensitivity to the other test gases in the temperature range from 600 to 800 °C. At 400 °C, an interesting selective response to NO in the concentration range from 1.5 to 2000 ppm is observed.

Consequently, the BFT30 ADM-coated thick film sensors may be used as temperature-independent oxygen sensors in exhausts between 700 and 900 °C. On the other hand, they can be used as NO sensors for air quality control applications at 400 °C, when the oxygen concentration remains constant.

Edited by: M. Penza
Reviewed by: two anonymous referees

References

Akedo, J.: Aerosol deposition of ceramic thick films at room temperature: densification mechanism of ceramic layers, J. Am. Ceram. Soc., 89, 1834–1839, 2006.

Akedo, J.: Room Temperature Impact Consolidation (RTIC) of Fine Ceramic Powder by Aerosol Deposition Method and Applications to Microdevices, J. Thermal Spray Technol., 17, 181–198, 2008.

Akiyama, M., Zhang, Z., Tamaki, J., Miura, N., and Yamazoe, N.: Tungsten oxide-based semiconductor sensor for detection of nitrogen oxides in combustion exhaust, Sensors and Actuators B: Chemical, 13–14, 619–620, 1993.

Alkemade, U. G. and Schumann B.: Engines and exhaust after treatment systems for future automotive applications, Solid State Ionics, 177, 2291–2296, 2006.

Bektas, M., Schönauer-Kamin, D., Hagen, G., Mergner, A., Bojer, C., Lippert, S., Milius, W., Breu, J., and Moos, R.: BaFe$_{1-x}$Ta$_x$O$_{3-\delta}$- a material for temperature independent resistive oxygen sensors, Sensors and Actuators B: Chemical, 190, 208–213, 2014.

Blase, R., Härdtl, K., and Schönauer, U.: Oxygen Sensor Based on Non-Doped Cuprate, United States Patent Specification, US 5, 792, 666, 1997.

Fergus, J. W.: Perovskite oxides for semiconductor-based gas sensors review, Sensors and Actuators B: Chemical, 123, 1169–1179, 2007.

Fleischer, M. and Meixner, H.: Oxygen sensing with long-term stable Ga$_2$O$_3$ thin films, Sensors and Actuators B: Chemical, 5, 115–119, 1991.

Gerblinger, J., Hauser, M., and Meixner, H.: Electric and Kinetic Properties of Screen-Printed Strontium Titanate Films at High Temperatures, J. Am. Ceram. Soc., 78, 1451–1456, 1995.

Huusko, J., Lantto, V., and Torvela, H.: TiO$_2$ thick-film gas sensors and their suitability for NOx monitoring, Sensors and Actuators B: Chemical, 15–16, 245–248, 1993.

Ivers-Tiffée, E., Härdtl, K. H., Menesklou, W., and Riegel, J.: Principles of solid state oxygen sensors for lean combustion gas control, Electrochimica Acta, 47, 807–814, 2001.

Kim, J. S., Hwang, I. S., Kim, S. J., Lee, C. Y., and Lee, J. H.: CuO nanowire gas sensors for air quality control in automotive cabin, Sensors and Actuators B: Chemical , 135, 298–303, 2008.

Lebedev, M., Akedo, J., and Ito, T.: Substrate heating effects on hardness of an α-Al$_2$O$_3$ thick film formed by aerosol deposition method, J. Crystal Growth, 275, e1301–e1306, 2005.

Marr, I., Groß, A., and Moos, R.: Overview on conductometric solid-state gas dosimeters, J. Sens. Sens. Syst., 3, 29–46, doi:10.5194/jsss-3-29-2014, 2014.

Menesklou, W., Schreiner, H. J., Härdtl, K. H., and Tiffée, E. I.: High temperature oxygen sensors based on doped SrTiO$_3$, Sensors and Actuators B: Chemical, 59, 184–189, 1999.

Merkle, R. and Maier, J.: How is oxygen incorporated into oxides? A comprehensive kinetic study of a simple solid-state reaction with SrTiO$_3$ as a model material, Angewandte Chemie-International Edition, 47, 3874–3894, 2008.

Moos, R., Rettig, F., Hürland, A., and Plog, C.: Temperature-independent resistive oxygen exhaust gas sensor for lean-burn engines in thick film technology, Sensors and Actuators B: Chemical, 93, 43–50, 2003.

Moos, R., Izu, N., Rettig, F., Reiß, S., Shin, W., and Matsubara, I.: Resistive Oxygen Gas Sensors for Harsh Environments, Sensors, 11, 3439–3465, 2011.

Moseley, P. T. and Williams, D. E.: Gas sensors based on oxides of early transition metals, Polyhedron, 8, 1615–1618, 1989.

Park, K. and Logothetis, E. M.: Oxygen sensing with Co$_{1-x}$Mg$_x$O ceramics, ECS J. Solid State Sci. Technol., 124, 1143–1446, 1977.

Penza, M., Martucci, C., and Cassano, G.: NOx gas sensing characteristics of WO$_3$ thin films activated by noble metals (Pd, Pt, Au) layers, Sensors and Actuators B: Chemical , 50, 52–59, 1998.

Riegel, J., Neumann, H., and Wiedenmann, H.-M.: Exhaust gas sensors for automotive emission control, Solid State Ionics, 152–153, 783–800, 2002.

Rettig, F., Moos, R., and Plog, C.: Poisoning of temperature independent resistive oxygen sensors by sulfur dioxide, J. Electroceram., 13, 733–738, 2004.

Sahner, K., Moos, R., Matam, M., Tunney, J., and Post, M.: Hydrocarbon sensing with thick and thin film p-type conducting perovskite materials, Sensors and Actuators B: Chemical, 108, 102–112, 2005.

Sahner, K., Straub, J., and Moos, R.: Cuprate-ferrate compositions for temperature independent resistive oxygen sensors, J. Electroceramics, 16, 179–186, 2006a.

Sahner, K., Moos, R., Izu, N., Shin, W., and Murayama, N.: Response kinetics of temperature-independent resistive oxygen sensor formulations: a comparative study, Sensors and Actuators B: Chemical, 113, 112–119, 2006b.

Sahner, K., Kaspar, M., and Moos, R.: Assessment of the novel aerosol deposition method for room temperature preparation of metal oxide gas sensor films, Sensors and Actuators B: Chemical, 139, 394–399, 2009.

Satake, K., Katayama, A., Ohkoshi, H., Nakahara, T., and Takeuchi, T.: Titania NOx sensors for exhaust monitoring, Sensors and Actuators B: Chemical, 20, 111–117, 1994.

Sayago, I., Gutiérrez, J., Arés, L., Robla, J. I., Horrillo, M. C., Getino, J., Rino, J., and Agapito, J. A.: The effect of additives in tin oxide on the sensitivity and selectivity to NOx and CO, Sensors and Actuators B: Chemical, 26–27, 19–23, 1995.

Schönauer, U.: Response times of resistive thick-film oxygen sensors. Sensors and Actuators B: Chemical, 4, 431–436, 1991.

Wiegleb, G. and Heitbaum, J.: Semiconductor gas sensor for detecting NO and CO traces in ambient air of road traffic, Sensors and Actuators B: Chemical, 17, 93–99, 1994.

Williams, D. E., McGeehin, P., and Tofield, B. C.: Oxygen Sensors, US Patent 4, 454–494, 1982.

Yu, C., Shimizu, Y., and Arai, H.: Investigation on a lean-burn oxygen sensor using perovskite-type oxides, Chem. Lett., 4, 563–566, 1986.

Zhou, X., Sørensen, O. T., and Xu, Y.: Defect structure and oxygen sensing properties of Mg-doped SrTiO$_3$ thick film sensors, Sensors and Actuators B: Chemical, 41, 177–182, 1997.